Role of potential structure in nonadiabatic collisions with applications to $He^+ + Ne(2p^6) \rightarrow He^+ + Ne(2p^53s)$ and $Na + I \rightarrow Na^+ + I^-$

D. A. Padmavathi and Manoj K. Mishra

Department of Chemistry, Indian Institute of Technology, Powai, Bombay 400076, India

Herschel Rabitz

Department of Chemistry, Princeton University, Princeton, New Jersey 08544

The first-order functional-sensitivity densities $\delta\sigma_{12}(E)/\delta V_{ij}(R)$ from close-coupling calculations are used for a quantitative probe of the role of structure in crossing diabatic curves used to model nonadiabatic collisions. Application to the excitation of Ne by He^+ shows a region of significance for $\delta\sigma_{12}(E)/\delta V_{12}(R)$ as a prominent Gaussian-like profile around the crossing point (R^*) in accord with the $\delta(R-R^*)$ idealization of the Landau-Zener-Stueckelberg (LZS) theory. Similarly, the densities $\delta\sigma_{12}(E)/\delta V_{11}(R)$ and $\delta\sigma_{12}(E)/\delta V_{22}(R)$ mimic $d\delta(R-R^*)/dR$-type behavior with one being the negative of the other in the neighborhood of R^*, in qualitative agreement with the LZS theory. However, all three sensitivity profiles identify a much broader area of importance for the curves than the loosely defined avoided-crossing region. Also, although the sensitivities themselves decrease with increasing energy, the domain of importance of the curves increases. Examination of the functional-sensitivity densities $\delta\sigma_{12}(E)/\delta V_{ij}(R)$ for the chemi-ionization collision $Na + I \rightarrow Na^+ + I^-$ reveals regions of potential-function importance very different from that predicted by the LZS theory. The chemi-ionization cross section is about ten times more sensitive to the ionic curve than the covalent curve. Also, the domain of sensitivity of the ionic curve is larger compared to that of the covalent curve. The density $\delta\sigma_{12}(E)/\delta V_{12}(R)$ for chemi-ionization shows that the area of maximum potential significance is not at the crossing point itself but the regions bracketing it on both sides. Also, the dominant sign dependence of the coupling sensitivity is unexpectedly negative. The results offer other observations about the domain of validity of the intuitive pictures rooted in the LZS theory. The significance of these results to the inversion of inelastic cross-section data is briefly discussed.

PACS number(s): 34.50.Pi, 34.20.Cf

I. INTRODUCTION

As a simple prototype of chemical reactions, the chemi-ionization reaction $Na + I \rightarrow Na^+ + I^-$ has received intense experimental and theoretical interest [1–3]. The dynamics of chemi-ionizations is controlled by the underlying potential-energy curves and coupling matrix elements. A quantitative knowledge of those regions of the curves controlling the dynamics is therefore of clear importance.

This dynamical dependence on the functional form of the underlying potential-energy curve(s) or surface(s) $V(R)$ may be examined through a first-order functional expansion of the collision cross section $\sigma([V])$,

$$\delta\sigma = \sigma([V+\delta V]) - \sigma([V]) \simeq \int dR \frac{\delta\sigma}{\delta V(R)} \delta V(R) , \quad (1)$$

where R denotes generic coordinate space variables.

The first-order functional-sensitivity density (derivative) $\delta\sigma/\delta V(R)$ serves the role of a weight function in Eq. (1). Those regions of R where $\delta\sigma/\delta V(R)$ is large imply regions of importance and the cross section is sensitive to changes in the potential(s) in this region. On the other hand, regions with small $\delta\sigma/\delta V(R)$ denote areas of the potential with little significance in the determination of the cross section. Additionally, the sign dependence

gives us a sense of how σ will respond to an increase or decrease in $V(R)$. While such an investigation may also be done using the brute-force method of varying $V(R)$ and repeating the calculations for the cross section many times, direct calculation of the functional sensitivities $\delta\sigma/\delta V(R)$ in the close-coupling approach requires only a minor extension and expense beyond the cross-section calculation [4] alone. This approach has been applied to determine regions of potential-energy curves critical to diverse dynamical processes [5].

In an earlier paper [6] we have employed the exponential distorted-wave (EDW) approximation to calculate the functional sensitivity densities $\delta\sigma_{12}(E)/\delta V_{ij}(R)$ for the collisional excitation $He^+ + Ne(2p^6) \rightarrow He^+ + Ne(2p^53s)$. The results obtained from this investigation showed the inadequacy of intuitive pictures of nonadiabatic collisions rooted in the Landau-Zener-Stueckelberg (LZS) theory [7]. The LZS theory continues to be used extensively for modeling nonadiabatic transitions using the crossing of the potential-energy curves corresponding to the participating states [1–3,8]. Although our earlier analysis [6] showed the limitations of the LZS theory, qualitatively correct behavior was found for the critical importance of the curve crossing point (R^*), the idealized LZS $\delta(R-R^*)$-type behavior for $\delta\sigma_{12}(E)/\delta V_{12}(R)$, and the $\pm d\delta(R-R^*)/dR$-type behavior for $\delta\sigma_{12}(E)/\delta V_{11}(R)$

and $\delta\sigma_{12}(E)/\delta V_{22}(R)$. The area of importance of all the potential-energy curves was, however, found to be much larger than the loosely defined avoided crossing region.

We attribute this qualitative success to the rather simple nature of the diabatic curves (as seen in Fig. 1) used to model the $He^+ + Ne(2p^6) \rightarrow He^+ + Ne(2p^53s)$ inelastic transition. Where there are competing features in the potential-energy curves it is not quite obvious how the significant regions can be intuited by any simple means including the LZS theory [e.g., the potential well followed by a distant crossing for chemi-ionization collisions $M + X \rightarrow M^+ + X^-$ (M is an alkali-metal atom, X is a halogen) or where fine-structure transitions, as in the $H^+ + F$ system, are mediated by adiabatic curves which do not cross but have competing features such as wells and humps [9,10]]. Also, the EDW and other perturbative approximations may not be suitable when coupling matrix elements are large, which is the case with the systems mentioned above. Moreover, for systems with long-range interactions, such as Na^+ and I^-, the EDW method can be quite expensive. It is, therefore, useful to develop tools for a rigorous and accurate calculation of the functional sensitivities without any approximation (except numerical integrations) for the treatment of the collision dynamics.

Recently, a compact formulation for the computation of functional-sensitivity densities of dynamical observables with respect to an arbitrary variation in the interaction potential has been presented [4], which employs the close-coupling method for calculation of collision cross sections. In the close-coupling approach to functional-sensitivity calculations, the wave functions already available from the scattering matrix-element calculations also determine the sensitivities. One can therefore have a rigorous calculation of both sensitivities and cross sections with just minor extensions to the close-coupling code.

In this paper, we present an adaptation of this approach to explore the role of structure in potential-energy curves and interaction matrix elements used to model nonadiabatic transitions. The nonadiabatic collisional excitation $He^+ + Ne(2p^6) \rightarrow He^+ + Ne(2p^53s)$ and ionization $Na + I \rightarrow Na^+ + I^-$ are used for illustration [1–3,6,11,12].

In Sec. II, we collect the theoretical and computational formulas needed for calculation of the close-coupling sensitivities. The results are discussed in Sec. III, and finally some concluding remarks are offered in Sec. IV.

II. THEORY

The assumption of only two electronic states along with a partial-wave expansion of the scattering functions for both states leads to the following coupled radial equations for the lth partial wave [13]:

$$\left[\frac{d^2}{dR^2} + k_i^2 - \frac{2\mu}{\hbar^2}V_{ii}(R) - \frac{l(l+1)}{R^2}\right]u_i^l(R)$$

$$= \frac{2\mu}{\hbar^2}V_{ij}(R)u_j^l(R), \quad i,j = 1,2 \ i \neq j \quad (2)$$

where

$$k_i^2 = \frac{2\mu}{\hbar^2}[E - V_{ii}(\infty)]$$

and $V_{ij}(R)$ is the usual diabatic matrix element between the electronic wave functions for the two states [14]. In Eq. (2) μ is the collisional reduced mass, R is the internuclear distance, and the radial scattering wave functions for the electronic states 1 and 2 are $u_1^l(R)$ and $u_2^l(R)$, respectively.

Alternatively the radial equations may be written in matrix form:

$$\left[\frac{d^2}{dR^2}\underline{I} + \underline{Q}\right]\underline{U} = \underline{0}, \quad (3)$$

where $\underline{U}$ is the solution vector, $\underline{I}$ is an $N \times N$ unit matrix, and $\underline{Q}$ is an $N \times N$ square matrix with elements

$$\underline{Q}_{ij} = \delta_{ij}\left[k_i^2 - \frac{l(l+1)}{R^2}\right] - \frac{2\mu}{\hbar^2}V_{ij}(R). \quad (4)$$

Numerical solution of the coupled equations proceeds by discretizing R into $M+1$ grid points R_i $\{i = 0, \ldots, M\}$ with R_0 sufficiently far in the nonclassical region and R_M in the asymptotic region. We have integrated the coupled equations using the renormalized Numerov method [4,15] where the ratio matrix for the regular solutions

$$\underline{R}_m = (\underline{U}_{m-1}^l)^{-1}\underline{U}_m^l \quad (m = 1, \ldots, M) \quad (5)$$

is propagated to the asymptotic region and then matched to

$$\underline{R}_M = [\underline{\mathcal{S}}_{M-1} - \underline{\mathcal{C}}_{M-1}\underline{K}][\underline{\mathcal{S}}_M - \underline{\mathcal{C}}_M\underline{K}]^{-1}, \quad (6)$$

where $\underline{\mathcal{S}}$ and $\underline{\mathcal{C}}$ are diagonal matrices of regular and irregular Riccati-Bessel functions as defined in Ref. [4]. (In Ref. [4], $\underline{\mathcal{S}}$ is denoted as Si and $\underline{\mathcal{C}}$ is denoted as Co.) The scattering matrix for each l may be obtained from the reactance matrix $\underline{K}$

$$\underline{S}^l = (\underline{1} + i\underline{K}^l)(1 - i\underline{K}^l)^{-1} \quad (7)$$

and the outgoing $(+)$ and incoming $(-)$ solutions for each partial wave have the form

$$\underline{U}_m^l \pm = \underline{U}_m^l[\underline{1} \mp i\underline{K}^l]^{-1}. \quad (8)$$

The total inelastic cross section $\sigma_{12}(E)$ is given by

$$\sigma_{1\rightarrow2} = \frac{\pi}{k_1^2}\sum_{l=0}^{\infty}(2l+1)|\underline{S}_{12}^l|^2, \quad (9)$$

whereby

$$\frac{\delta\sigma_{12}(E)}{\delta V_{ij}(R)} = \frac{\pi}{k_1^2}\sum_l(2l+1)\text{Re}\left[[\underline{S}_{12}^l(E)]\frac{\delta\underline{S}_{12}^l(E)}{\delta V_{ij}(R)}\right]. \quad (10)$$

It has been shown [4] that

$$\frac{\delta S_{1\rightarrow2}(E)}{\delta V_{ij}(R)} = -2\pi i\langle 2,E-|R,i\rangle\langle j,R|1,E+\rangle \quad (11)$$

where $\langle 2,E-|R,i\rangle$ denotes the complex conjugate of the

*i*th component of the incoming $(-)$ wave in channel 2 and $\langle j,R\,|\,1,E+\rangle$ denotes the *j*th component of the outgoing $(+)$ wave in channel 1.

Let R_n be the *n*th point on the solution. Grid then using Eqs. (8) and (11) we have

$$\frac{\delta\sigma_{12}(E)}{\delta V_{ij}(R_n)}=\frac{4\pi}{k_1^2}\sum_l (2l+1)\mathrm{Im}[(\underline{S}^l_{12})^*\underline{U}^{l+}_n(i,2)$$

$$\times\underline{U}^{l+}_n(j,1)]\ . \qquad (12)$$

This serves as our working equation for the computation of sensitivities reported in this paper.

III. RESULTS AND DISCUSSION

The log-normalized functional-sensitivity derivatives $\delta\ln\sigma_{12}(E)/\delta\ln V_{ij}(R)$ can assess the *relative* importance of different potential-energy curves as well as that of different regions in these curves to the collision cross section. Using log-normalized functional-sensitivity densities, we can easily determine if the cross section is more sensitive to variations in a particular potential-energy curve or whether the coupling matrix element is the more important input. Before applying the log-normalized close-coupling sensitivity derivatives to complicated problems beyond the reach of the previously employed EDW approximation, we reexamine the simple collisional excitation of Ne by He$^+$, amenable to both approaches.

The collisional excitation of Ne by He$^+$ is modeled by the crossing of two diabatic curves shown in Fig. 1. The functional form and modeling parameters (in a.u.) are those formulated by Olsen and Smith [11(a)], where

$$V_{11}(R)=21.1R^{-1}\exp(-R/0.678)\ , \qquad (13)$$

$$V_{22}(R)=(21.1R^{-1}-12.1)\exp(-R/0.678)+0.6174\ , \qquad (14)$$

$$V_{12}(R)=0.170\exp(-R/0.667)\ , \qquad (15)$$

and have been used in previous calculations [6,11,16,17]. The crossing curves used to model the chemi-ionization Na+I$\rightarrow$Na$^+$+I$^-$ are plotted in Fig. 2. The functional form and modeling parameters (in Å and eV) given below;

$$V_{11}(R)=[3150+(2.647/R)^{12}]$$

$$\times\exp(-R/0.435)-1000/R^6\ , \qquad (16)$$

$$V_{22}(R)=[2760+(2.398/R)^8]\exp(-R/0.3489)$$

$$-(e^2/R)-(6.839e^2/2R^4)-11.3/R^6$$

$$-(2e^2\times0.408\times6.431)/R^7+2.075\ , \qquad (17)$$

$$V_{12}(R)=17.08\exp(-R/1.239) \qquad (18)$$

are those formulated by Faist and Levine [12(a)] and used by others [1,2,12(c)]. Although $V_{12}(R)$ is similar for both cases, the potentials $V_{ii}(R)$ are quite distinct. Accordingly, the regions of potential-function significance will be found below to be very different.

A. He$^+$+Ne

We present only a brief treatment of the nonadiabatic transition He$^+$+Ne$(2p^6)\rightarrow$He$^+$+Ne$(2p^53s)$ as it was studied earlier using the more approximate but qualitatively correct EDW method. Apart from providing insights for this system, the close-coupling sensitivity profiles for He$^+$+Ne can provide a good reference to better appreciate the significance of the Na+I results. The close-coupling cross sections are compared with those from other theoretical approaches in Table I. The perturbative approaches are known to often overestimate total inelastic cross sections as found here. The log-normalized functional sensitivities are plotted in Figs. 3 and 4.
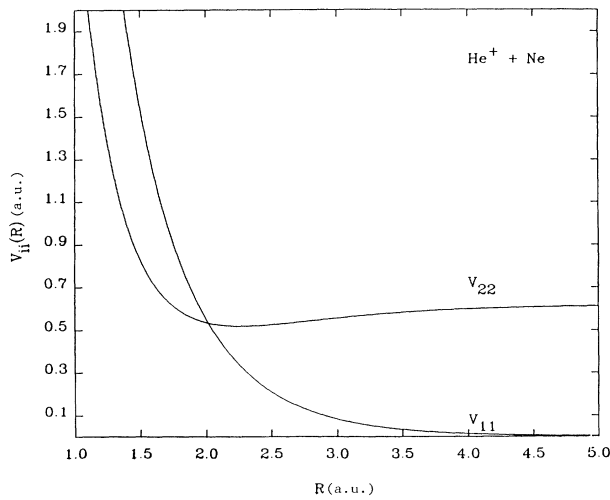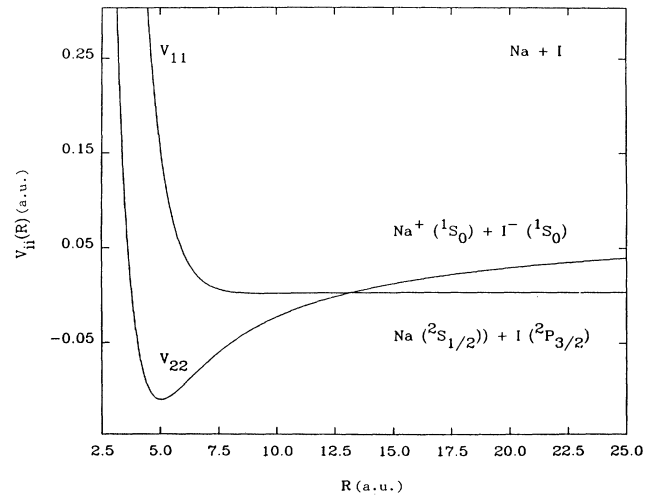

FIG. 1. The diabatic potentials $V_{11}(R)$ and $V_{22}(R)$ for collisional excitation of Ne by He$^+$. The curves cross at $R^*=2.02a_0$. The functional forms and the corresponding parameters for the potentials and the coupling matrix element $V_{12}(R)$ are from Ref. [11(a)].

FIG. 2. Diabatic potential-energy curves for Na+I. The functional form and parameters are those from Ref. [12(a)]. The crossing point R^* is at $13.2a_0$.

TABLE I. Total excitation cross sections for $He^+ + Ne$. All values are in atomic units.

| Energy | Cross section | | | |
	Present calculation	EDW (Ref. [6])	DW [Ref. [11(a)]]	UWKB [Ref. [11(d)]]
0.919	0.785	0.820	0.874	
1.000	0.822	0.842		0.873
1.500	0.785	0.818		0.844
2.000	0.746	0.765		0.779
2.600	0.675	0.709		0.719
2.606	0.672	0.706	0.729	

Just as in the earlier EDW analysis [6], clear qualitative similarity exists between the Gaussian-like profile for $\delta\sigma_{12}(E)/\delta V_{12}(R)$ in Fig. 3 centered at the crossing point R^* and the idealized LZS $\delta(R - R^*)$-type behavior; in addition, the behavior in Fig. 4 of $\delta\sigma_{12}(E)/\delta V_{11}(R) \simeq -\delta\sigma_{12}(E)/\delta V_{22}(R)$ near $R \simeq R^*$ and their derivativelike slope is again reflective of the idealized $\pm d\delta(R - R^*)/dR$ result from the LZS theory. Thus the magnitude of $V_{12}(R)$ and slopes of $V_{11}(R)$ and $V_{22}(R)$ near the crossing point are key physical variables [6]. The fact that the region of importance for all three curves $V_{11}(R)$, $V_{22}(R)$, and $V_{12}(R)$ is much larger than the loosely defined avoided crossing region clearly demonstrates the need to go beyond the LZS theory. Quantitative comparisons may be made by calculating the static width (Δx_s) and dynamic width (Δx_d)

$$\Delta x_s = 2V_{12}/|F_1 - F_2| , \qquad (19)$$

$$\Delta x_d = v/(2|F_1 - F_2|)^{1/2} \qquad (20)$$

of the transition region associated with the LZS theory [13], where F_1 and F_2 are the slopes of the diabatic potentials $V_{11}(R)$ and $V_{22}(R)$, v is the relative velocity, and all the quantities are evaluated at the crossing point R^*. The width of the effective transition zone is defined as the larger of the two quantities Δx_s and Δx_d. For the cases considered here, $\Delta x_s \ll \Delta x_d$, e.g., for the collisional excitation of Ne by He^+ at $E = 2.606$ a.u., $\Delta x_s = 0.019$ a.u., while $\Delta x_d = 0.18$ a.u. It is the dynamic width which controls the extent of the LZS transition region. This width is marked in Figs. 3, 4, and 6–8 and clearly demonstrates that the region of significance of these curves is much larger than that predicted by the LZS theory.

The use of log-normalized functional derivatives allows a comparison of the *relative* importance of the various curves and it is clear from Fig. 3 that both the potential-energy curves are equally important, over the same
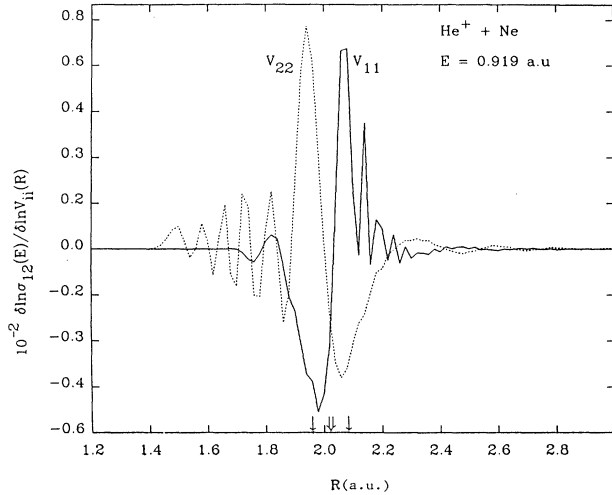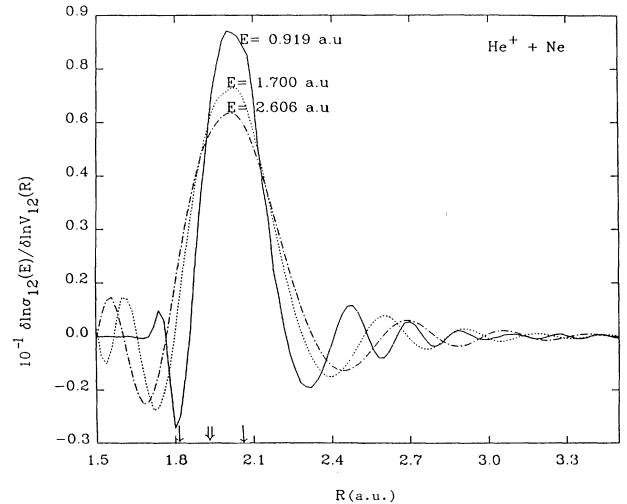

FIG. 3. Log-normalized sensitivity profiles $\delta\ln\sigma_{12}(E)/\delta\ln V_{11}(R)$ and $\delta\ln\sigma_{12}(E)/\delta\ln V_{22}(R)$ at $E = 0.919$ a.u. for $He^+ + Ne$. The correlated $\pm d\delta(R - R^*)/dR$ qualitative behavior for $V_{11}(R)$ and $V_{22}(R)$ sensitivities in the vicinity of $R^*(\parallel)$ is consistent with the LZS theory. The magnitude of these sensitivities is almost the same and the domain of importance is much larger than the dynamic width of the transition region Δx_d (the interval between the two $\parallel$ arrows) prescribed by the LZS theory. The static width Δx_s is much too small to be displayed.

FIG. 4. Log-normalized sensitivity profile $\delta\ln\sigma_{12}(E)/\delta\ln V_{12}(R)$ for $He^+ + Ne$ at different total energies. The Gaussian-type feature centered at $R^*(\parallel)$ mimics the idealized LZS $\delta(R - R^*)$ behavior. The interval between the two $\downarrow$ arrows is the dynamic width Δx_d calculated at $E = 2.606$ a.u. The domain of sensitivity extends far beyond the transition region specified by the LZS theory and underscores the need to augment the intuitive pictures rooted in the LZS theory.
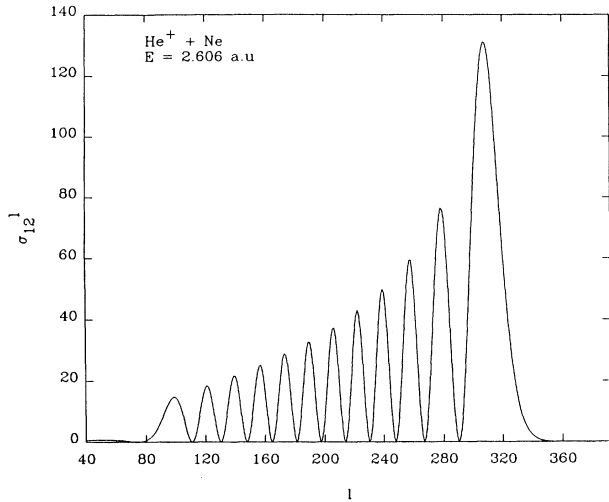
FIG. 5. Plot of partial cross sections $\sigma_{12}^l = (2l+1)|S_{12}^l|^2$ as a function of l for $E = 2.606$ a.u. The plot is in agreement with those from Refs. [11(a)] and [11(b)]. Taking $R = l/k_2$ we estimate the domain of sensitivity to be 0.6–2.4 a.u. in reasonable agreement with that seen in sensitivity plots (Figs. 3 and 4). Taking $l^* \simeq k_2 R^*$ we get $l^* = 314$, in excellent agreement with the l value for the maximum in the σ_{12}^l profile.

domain of R values centered at R^*. Comparison of Figs. 3 and 4 reveals that the collision cross section is about an order of magnitude more sensitive to the potential-energy curves than to the coupling matrix element, in accord with the weak-coupling between the two states. This weak dependence on coupling also explains why the EDW approximation is so successful in this case. The success of a reported semiclassical inversion procedure [17] in inverting the differential inelastic cross section for He$^+$+Ne to obtain the coupling matrix element, we speculate, may also be attributed to this serendipity. In the case of systems with strong coupling, we expect that the more general inversion procedure based on functional-sensitivity coefficients [18] will be necessary.

In Fig. 5, we have plotted the partial cross sections $\sigma_{12}^l = (2l+1)|\underline{S}_{12}^l|^2$ as a function of l for He$^+$+Ne at $E = 2.606$ a.u. The plot is in general agreement with those from Refs. [11(a)] and [11(b)]. Taking $l \simeq k_2 R$, the regions of importance in σ_{12}^l vs l profile of Fig. 5 may be approximately translated into internuclear distances of significance to the collision cross-section. With this estimation procedure we get the domain of sensitivity to be approximately 0.6–2.4 a.u., in reasonable agreement with that seen in the sensitivity plots (Figs. 3 and 4). Taking $l' \simeq k_2 R^*$, we get $l^* = 314$, in excellent agreement with the l value for the maximum in the σ_{12}^l profile.

B. Na+I

The chemi-ionization cross sections at energies of interest to our functional sensitivity analysis of Na+I→Na$^+$+I$^-$ are collected in Table II. These compare favorably with the results of an earlier close-

TABLE II. Total ionization cross sections for Na+I. All values are in atomic units.

Energy	Cross section	
	Present calculation	Ref. [12(a)]
0.3	157.41	160.0
0.9	240.77	245.0
1.5	267.67	270.0

coupling calculation [12(a)], where for most l values, an approximate JWKB-based interpolation was used to compute $\underline{S}_{12}^l$. The present results are from fully converged close-coupling calculations, insensitive to further refinements of the mesh or extension of the asymptotic regime, for each partial wave. For the ionic channel, the Coulomb potential was effectively screened at large R, thus permitting the use of the boundary condition in Eq. (6). The functional-sensitivity derivatives for the chemi-ionization are displayed in Figs. 6–8. In Fig. 6 we have plotted to unnormalized functional sensitivity profile $\delta\sigma_{12}(E)/\delta V_{11}(R)$ for NaI at $E = 0.3$ a.u. The derivative of a δ-function-type feature around R^* in Fig. 6 is distorted but apparent. However, to compare the magnitudes of sensitivities for different potential-energy curves and at different energies, the log-normalized profiles are required. These heighten the importance of the small-R region of the curve over the $V_{22}(R)$ well as a result of the rapid increase in the value of $V_{11}(R)$ for small R. The high-frequency oscillations at small R in Fig. 6 are associated with the effective wave vector $k_2(R) = \sqrt{(2\mu/\hbar^2)[E - V_{22}(R)]}$ being very large there. In contrast, $k_1(R)$ actually decreases as R decreases due to the repulsive shape of $V_{11}(R)$. The fact that the
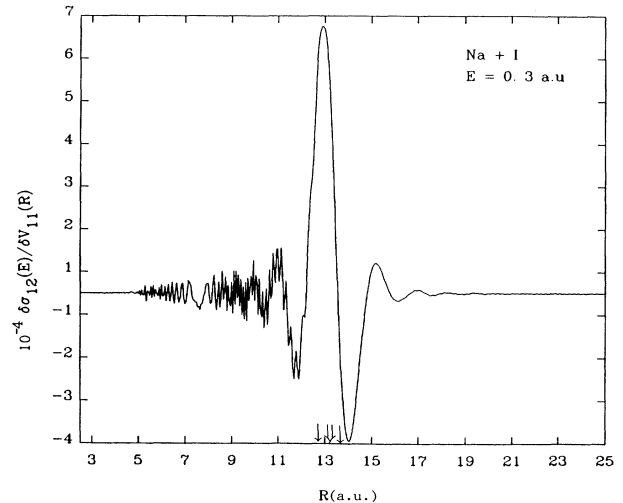

FIG. 6. Functional sensitivity profile $\delta\sigma_{12}(E)/\delta V_{11}(R)$ for Na+I at $E = 0.3$ a.u. Only a remnant of the first-derivative-type feature around R^*(⇂) is apparent. The strong oscillations at small R are due to the dominant influence of V_{22} upon the dynamics with V_{11}. The interval between the two ↓ arrows in the effective transition region calculated from the LZS theory. Conclusions from Figs. 3 and 4 apply.

$\delta\sigma_{12}(E)/\delta V_{11}(R)$ at small R reflects distinct $V_{22}(R)$ behavior is a result of the strong coupling $V_{12}(R)$ in the crossing point region. The nearly symmetric $\pm$ ringing at small R in Fig. 6 implies that a smooth variation $\delta V(R)$ in this region will not significantly reflect this behavior in the cross section. Hence we can focus on the behavior at large R in Fig. 6.

In Fig. 7 we have plotted the log-normalized functional-sensitivity profiles $\delta\ln\sigma_{12}(E)/\delta\ln V_{ii}(R)$, $i=1,2$, for Na+I at $E=0.3$ a.u. It is clear that the chemi-ionization cross section is much more sensitive to the ionic curve $V_{22}(R)$ and also over a much larger range of internuclear distances compared to the covalent curve $V_{11}(R)$ in keeping with the strong long-range Coulombic nature of the interaction $V_{22}(R)$. That this comparative importance of $V_{22}(R)$ with respect to $V_{11}(R)$ persists at other energies as well.

Log-normalized functional-sensitivity profiles $\delta\ln\sigma_{12}(E)/\delta\ln V_{12}(R)$ for NaI at different collisional energies are plotted in Fig. 8. Instead of the *positive* Gaussian-like structure centered at R^* expected from the LZS theory and seen for $He^+ + Ne$ in Fig. 3, we see a complex form best described as a dominantly *negative* feature centered not quite at the R^* for Na+I. Also, the domain of sensitivity is much larger than that for $He^+ + Ne$ in keeping with the much wider strong-coupling regime for chemi-ionization as opposed to collisional excitation. The sensitivity to coupling decreases with an increase in collisional energy but remains substantial over the energy domain considered here. Comparison of Figs. 7 and 8 reveals that in the strong-coupling case of Na+I, the sensitivity of the ionization cross section to the coupling matrix element $V_{12}(R)$ is
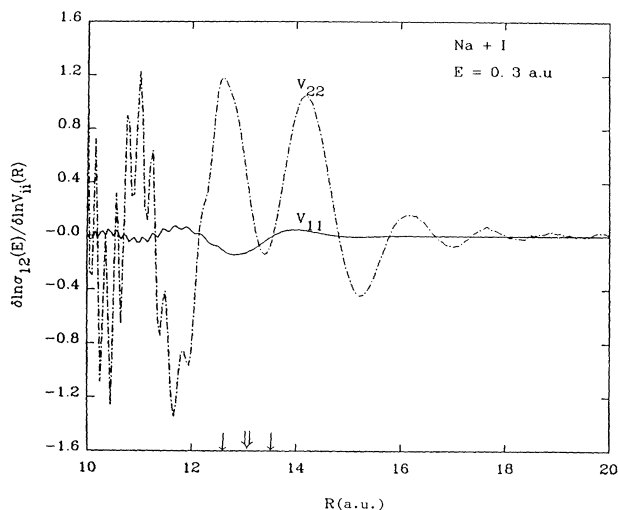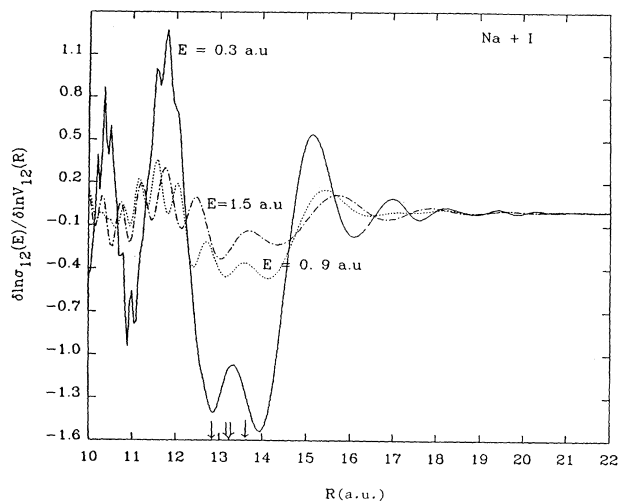
FIG. 8. Log-normalized functional sensitivity profiles $\delta\ln\sigma_{12}(E)/\delta\ln V_{12}(R)$ for Na+I at different collisional energies. Instead of a *positive* Gaussian-like feature centered at $R^*(\,\|\,)$, predicted by the LZS theory, we see a complex pattern of potential significance dominated by a *negative* feature not quite at R^*. Also, the domain of sensitivity is very wide in keeping with the much broader strong-coupling regime for chemi-ionization here. The sensitivity to coupling decreases with an increase in collisional energy but remains substantial over the energy domain considered here. The width of the transition region predicted by the LZS theory (the interval between the two $\downarrow$ arrows) is far too small.

comparable to that for $V_{22}(R)$ with both these potential-energy curves being much more important to the collision outcome than the rather flat covalent curve $V_{11}(R)$. The partial cross sections $\sigma_{12}^l=(2l+1)|\underline{S}\,_{12}^l|^2$ as a function of l for Na+I appear qualitatively similar to Fig. 5. The domain of sensitivity and the maximum in σ_{12}^l profile once again correlate excellently with the region of potential significance and R^* obtained from the sensitivity curves for NaI.

The static width $\Delta x_s = 0.142$ a.u. is about an order of magnitude larger than that for collisional excitation of Ne by He^+ due to the long range and large strength of the Coulombic coupling. The dynamic width Δx_d at $E=0.3$ a.u. is 0.85 a.u. and again controls the range of the effective LZS transition region marked in Figs. 6–8. The quantitative inadequacy of the intuitive pictures rooted in the simple LZS theory is obvious.

The $V_{ii}(R)$ sensitivity behavior near the crossing region in Na+I is radically different from that found in the $He^+ + Ne$ system where quasi-LZS structure was found. In the stronger coupled Na+I case extensive mixing has all but obscured the expected slope dependence on $V_{ii}(R)$ and the detailed way in which the collision draws on $V_{ii}(R)$ cannot be intuited on any simple grounds. The same conclusion should be true for other strongly coupled curve-crossing systems.

IV. CONCLUDING REMARKS

In this paper, functional-sensitivity derivatives were employed to gain insights into comparative importance of

FIG. 7. Log-normalized functional sensitivity profiles $\delta\ln\sigma_{12}(E)/\delta\ln V_{11}(R)$ and $\delta\ln\sigma_{12}(E)/\delta\ln V_{22}(R)$ for Na+I at $E=0.3$ a.u. It is clear that the chemi-ionization cross section is much more sensitive to the ionic curve $V_{22}(R)$ and also over a much larger range of internuclear distances compared to the covalent curve $V_{11}(R)$ in keeping with the Coulombic nature of the interaction $V_{22}(R)$. The domain of sensitivity is much larger than the LZS dynamic width Δx_d (the interval between the two $\downarrow$ arrows) centered at the crossing point ($\|$).

various potential-energy curves and coupling matrix elements mediating a nonadiabatic collision. Although the results for $He^+ + Ne$ can be understood qualitatively from the LZS theory, their quantitative details cannot be ascertained. In contrast for the stronger coupled $Na + I$ system, identification of which parts of the potentials are important cannot be intuited *a priori*. Moreover, while for the nonadiabatic collisions described by curves which cross, one can still guess that the region around the crossing is the most important, no such prior insight can be had where the mediating curves do not cross (e.g., the case of collisional fine-structure transitions [9,10] in F or where there are multiple crossings [8,19,20]). The fact that a plot of partial cross section $\sigma_{12}^l = (2l + 1)|\underline{S}_{12}^l|^2$ as a function of l effectively elicits the domain of sensitivity is of help, but it cannot offer any clues to the *relative* importance of the underlying curves. We therefore conclude that very interesting and possibly counterintuitive conclusions may result from a careful sensitivity analysis of fine-structure transitions and multicurve-crossing problems. This information may be further employed in an iterative fashion as the kernel of an inversion algorithm to systematically extract potentials from appropriate laboratory data [18]. An algorithm utilizing informations from both differential and total cross-section sensitivities shall greatly assist in this task. An effort along these latter lines is underway.

[1] A. H. Zawail, Nature **348**, 225 (1990), and references therein.

[2] H. Metiu and V. Engel, J. Opt. Soc. Am. B **7**, 1709 (1990), and references therein.

[3] R. D. Levine and R. B. Bernstein, *Molecular Reaction Dynamics and Chemical Reactivity* (Oxford University Press, New York, 1987).

[4] S. Shi and H. Rabitz, Comput. Phys. Rep. **10**, 1 (1989).

[5] M. J. Smith, S. Shi, and H. Rabitz, J. Chem. Phys. **91**, 1051 (1987).

[6] M. Mishra, R. Guzman, and H. Rabitz, Phys. Rev. A **36**, 1124 (1987).

[7] L. Landau, Sov. Phys. **2**, 46 (1932); C. Zener, Proc. R. Soc. London, Ser. A **137**, 696 (1933); E. C. G. Stueckelberg, Helv. Phys. Acta **5**, 369 (1932).

[8] H. Nakamura, J. Chem. Phys. **87**, 4031 (1987); H. Nakamura, J. Phys. Chem. **88**, 4812 (1984); M. H. Alexander, in *Gas Phase Chemiluminescence and Chemi-Ionization*, edited by A. Fontijn (Elsevier, New York, 1985); M. S. Child, in *Specialist Periodical Reports, 2, Molecular Spectroscopy* (Chemical Society of London, London, 1974).

[9] P. S. Julienne, M. Krauss, and A. C. Wahl, Chem. Phys. Lett. **11**, 16 (1971).

[10] F. H. Mies, Phys. Rev. A **3**, 942 (1973).

[11] (a) R. E.Olson and F. T. Smith, Phys. Rev. A **3**, 1607 (1971); (b) J. P. Braga, L. J. Dunne, and J. N. Murrell, Chem. Phys. Lett. **120**, 147 (1985); (c) M. S. Child and R. B. Gerber, Mol. Phys. **38**, 421 (1979); (d) B. C. Eu and T. P. Tsien, Phys. Rev. A **7**, 648 (1973).

[12] (a) M. B. Faist and R. D. Levine, J. Chem. Phys. **64**, 2953 (1976); (b) M. C. Moutinho, J. A. Aten, and J. Los, Physica **67**, 166 (1973); (c) R. Grice and D. Herschbach, Mol. Phys. **27**, 159 (1974); (d) S. H. Schaefer, D. Bender, and E. Tiemann, Chem. Phys. **89**, 65 (1984).

[13] M. S. Child, *Molecular Collision Theory* (Academic, London, 1974).

[14] F. T. Smith, Phys. Rev. **179**, 111 (1969); S. A. Evans, J. S. Cohen, and N. F. Lane, Phys. Rev. A **4**, 2235 (1971).

[15] B. R. Johnson, J. Chem. Phys. **69**, 4678 (1978).

[16] R. E. Langer, Phys. Rev. **51**, 669 (1937); W. D. Smith and R. T. Pack, J. Chem. Phys. **70**, 4609 (1979).

[17] M. S. Child and R. B. Gerber, Mol. Phys. **38**, 421 (1979).

[18] T.-S. Ho and H. Rabitz, J. Chem. Phys. **89**, 5614 (1988); **91**, 7590 (1989); **94**, 2305 (1991).

[19] Y. Sun and A. Dalgarno, J. Chem. Phys. **96**, 5017 (1992).

[20] D. A. Padmavathi, M. K. Mishra, and H. Rabitz, Phys. Rev. A **48**, 286 (1993).